Disclinations of monolayer graphite and their electronic states

Ryo Tamura and Masaru Tsukada
Department of Physics, Faculty of Science, University of Tokyo, Hongo 7-3-1, Bunkyo-ku, Tokyo 113, Japan
(Received 23 July 1993)

The local density of states (LDOS) of a single disclination and a disclination pair of various configurations in the monolayer graphite is calculated by the recursion method introduced by Haydock [J. Phys. C **5**, 2845 (1972)]. The LDOS shows the existence of some resonant states near the Fermi energy. At the Fermi level, the value of the LDOS vanishes for a single disclination of five- and seven-membered rings, and remains a finite value for four- and eight-membered rings. On going away from the disclination center, the shape of the LDOS approaches that of the perfect lattice. At the Fermi level, a sharp peak structure, which corresponds to a localized state, appears in the LDOS of fused disclinations consisting of a four-membered ring and a seven-membered ring, and the value of the LDOS vanishes in the case of fused disclinations consisting of two five-membered rings. But these features are drastically changed if the configuration of the disclination pair satisfies a certain simple condition. Using the fact that the Fermi level of these systems with disclinations is the same as that of the perfect monolayer graphite, the charge and the stability energy at each site are calculated from the LDOS. We show that the disclination center of a five-membered ring has a negative charge, that of a seven-membered ring has a positive charge, and that of an even membered ring is neutral.

I. INTRODUCTION

Recently, various kinds of exotic materials made of closed curved surfaces of graphite layers have been found, and their unique properties have attracted much interest. They include fullerene, carbon nanotubes, and others.[1] A perfect planar graphite layer has the form of honeycomb network; its structure is characterized by a six-membered ring of carbon atoms. To make a curved surface from a graphite layer, other types of carbon rings, i.e., n-membered rings with n different from six, have to be introduced in the graphite layer. For example, according to Euler's theorem on polyhedra, a closed surface of a graphite layer includes 12 five-membered rings in addition to any number of six-membered rings. This is clearly demonstrated by the actual structure of fullerenes and capped nanotubes.[2] On the other hand, at the joining part of the carbon nanotubes with different diameters, there should be a saddle point which is formed by an $n(>6)$-membered ring.[3]

The special portion of the curved graphite layer characterized by $n(\neq 6)$-membered ring(s) corresponds to a disclination center in the otherwise perfect two-dimensional (2D) periodic lattice structure of the graphite. This is illustrated in Fig. 1. A disclination is a topological defect; local geometry at any sites around the disclination is completely the same as that of the perfect lattice, i.e., each atom is connected to three nearest-neighbor atoms. It exerts some influence on the electron wave function, only when an electron wave splits into two before encountering the disclination, and combines again to be a single wave function after passing it. Therefore the change of the local electronic structure induced by the disclination is not a trivial problem, and much more complicated than the effect by a local potential, e.g., by an impurity center. Thus the investigation of electronic states due to topological disorder has attracted much interest from theorists. For example, dislocation has been studied by Irie and Kawamura, with an analogy model to the Aharonov-Bohm effect.[4]

Moreover, for the case of the 2D graphite, there is particular interest in the effect around the Fermi level, E_F, because of the degenerate band states and the cusp-

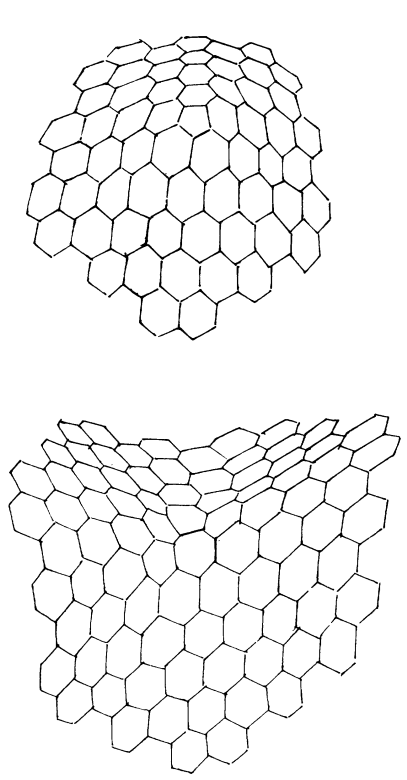

FIG. 1. The shape near a disclination center; (a) for a five-membered ring, and (b) for a seven-membered ring.

shaped density of states at the K point in the Brillouin zone. It is expected that the situation is drastically different from the free-electron systems which were studied recently by Nagaoka and Ikegami.[5] They found that the effect of the kinetic energy normal to the surface appears as an effective potential for the electrons confined in a curved 2D surface. Our interest in this paper is focused on the topological aspect related to the lattice structure, and is quite different from the problems of the free electron. Our calculation takes into account only how atoms are connected, and the effect of the curvature of the surface is not a major concern. Kitahara, Araki, and Nakazato studied the diffusion of a particle on a curved surface, and derived the Fokker-Plank equation that has an effective potential which either enhances or reduces the diffusion.[6] In this calculation, the effective potential appears as an effect of a topological disorder.

Studying the local change of the electronic structure induced by the disclination is of interest as a search for a general property characteristic of closed curved graphite surfaces. It is possible that the growth process of carbon nanostructures is initiated from such a disclination center, because it tends to act as a chemical reaction center.[7] Moreover, new functions of these nanostructures in electronic devices are related to special electronic states around singular points.

II. MODEL AND METHOD FOR THE CALCULATION

We investigate the electronic properties of disclination by means of the recursion method introduced by Haydock.[8] In this method, one can calculate the local density of states (LDOS) for any tight-binding system with infinite size without assuming artificial finite models as clusters or supercell structures. The only required condition is that the structure is unambiguously designated with a definite rule. Therefore this method is most convenient for the description of scattering states.

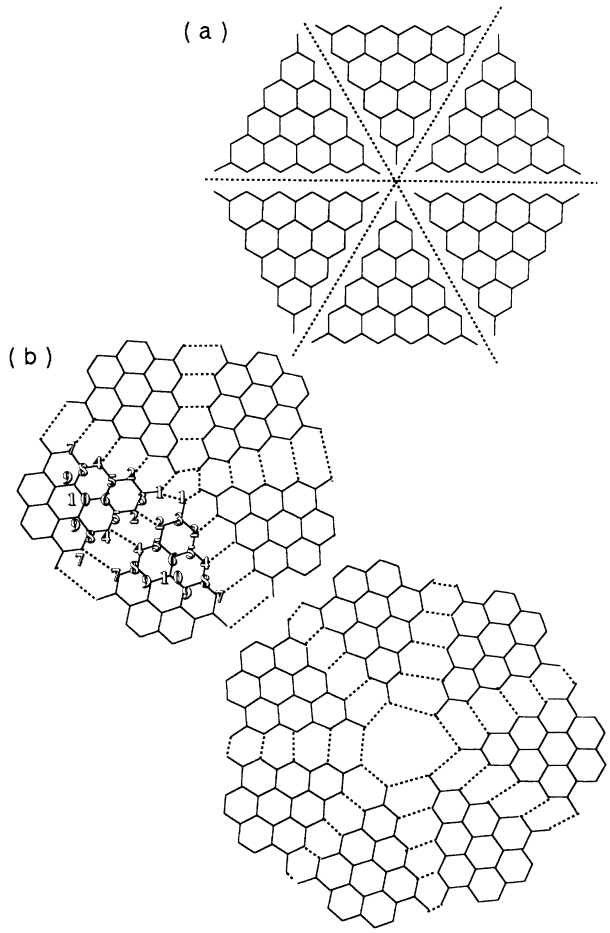

FIG. 2. (a) Six sectors divided from the perfect graphite lattice. (b) A 5 system and a 7 system. An n system is formed by connecting n sectors. For an n system, the $2n$ equivalent sites are sites 2, 4, 5, 7, 8, and 9, and the n equivalent sites are 1, 3, 6, and 10.

A. Model for the calculation

To construct a model for disclination(s) in a graphite layer, we adopt the following procedure: from the center of a six-membered ring in a perfect monolayer graphite, we draw three linear lines at 120° to each other, which run through centers of the C-C bonds of the innermost hexagon [see Fig. 2(a)]. By these lines the whole plane is divided into six sectors.

An n-membered ring can be formed either by removing $6-n$ sectors (if $n<6$), or inserting $n-6$ sectors (if $n>6$). At the boundary of the sectors, a carbon atom on one side of the sector is bonded to the nearest-neighboring carbon atom in the adjacent sector in a natural way. In the case of $n<6$, the n-membered ring becomes a top of a conical shape, and in the case of $n>6$ it becomes a center of the saddle point (see Fig. 1). For example, Fig. 2(b) shows this procedure for the case of $n=5$ and 7. From now on, we shall call such a system an n system.

It is also easy to form a system which contains two disclinations, an n-membered ring and an m-membered ring, which will be called an n-m system hereafter. The configuration is described by the vector that joins the two disclination centers, $i\mathbf{e}_1+j\mathbf{e}_2$, and will be represented by (i,j) hereafter (see Fig. 3). An n-7 system is formed by connecting $n+1$ sectors as below. We connect n sectors in the same way as in the case of the single disclination discussed above, but connect the last sector after shifting it by i sites in the radial direction. There are $i-1$ hexagons between the n-membered ring and the seven-membered ring, so its configuration is $(i,0)$. Examples are shown in Fig. 4(c) for the case of $n=4$ and $i=1$. We introduce a sector which has the shape of a trapezoid for the purpose of forming an n-5 system. It can be done by connecting $n-1$ isosceles triangle sectors and one trapezoid sector, as shown in Fig. 5. The number of hexagons between the n-membered ring and the pentagon can be changed by changing the size of the trapezoid sector (see Fig. 5 in the case of $n=5$). The configurations of the systems shown in Figs. 5(a), 5(b), and 5(c) are (1,0), (2,0), and (3,0), respectively. For the case of the configuration (i,j), where neither i nor j is zero, it is also possible to form an n-m system by connecting such sectors appropriately. By a simple geometrical rule connecting C-C

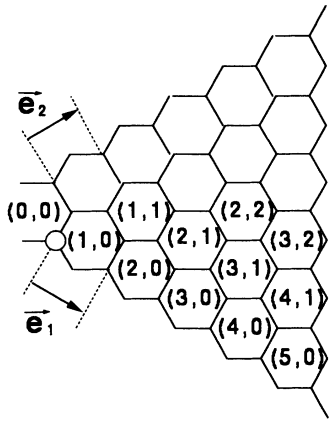

FIG. 3. The label to define configuration of two disclination centers. The position of the n-membered ring disclination center is taken as (0,0), and the position of the m-membered ring disclination center is represented by (i,j). Here (i,j) means position vector $i\mathbf{e}_1+j\mathbf{e}_2$, where both i and j are integers.

bonds between each sectors, one can easily generate the coefficients of the recursion formula.

B. Recursion method

In this section we give a brief summary of Haydock's recursion method, details of which are given in Ref. 8.

First, it is easy to number every site of each sector. The carbon $2p_z$ orbital at site i will be indicated by $|i\rangle$, and for simplicity these are assumed to form an orthogonal normalized set. In the real system, the $2p_z$ orbital is mixed with the σ orbital, because the system is not on a flat plane. However, for simplicity, this effect is ignored. The assumption is reasonable when the radius of the curvature of the graphite layer is large. We choose the origin of energy as the common site energy $\langle i|H|i\rangle$, and assume the matrix elements of the Hamiltonian to be

$$\langle i|H|j\rangle=\begin{cases}-T & \text{if } i \text{ and} j \text{ are nearest neighbors}\\ 0 & \text{otherwise .}\end{cases}$$

In the following, the value of T is constant and treated as the unit of energy, that is, $T=1$. The index 0 is assigned to the site where we want to obtain the LDOS, $N_0(E)$. Then $N_0(E)$ is obtained from the Green's function $G_{ij}(E)$

$$G_{ij}(E)\overset{\text{def}}{=}\langle i|(E-H)^{-1}|j\rangle \tag{1}$$

as

$$N_0(E)=\lim_{\delta\to+0}\frac{1}{\pi}\mathrm{Im}G_{00}(E-i\delta)\ . \tag{2}$$

Here i is the unit of imaginary number, Im is the imaginary part, and δ is a positive infinitesimal.

We can obtain $G_{00}(E)$ from the moment μ_m,

$$\mu_m\overset{\text{def}}{=}\langle 0|H^m|0\rangle=\sum_{a,b,\ldots,f}\langle 0|H|a\rangle\langle a|H|b\rangle\cdots\langle f|H|0\rangle\ , \tag{3}$$

by the relation

$$\begin{aligned}G_{00}(E)&=\langle 0|E^{-1}\left[1-\frac{H}{E}\right]^{-1}|0\rangle\\&=\langle 0|E^{-1}\left[1+\sum_{m=1}^{\infty}\frac{H^m}{E^m}\right]|0\rangle\\&=E^{-1}\left[1+\sum_{m=1}^{\infty}\frac{\mu_m}{E^m}\right]\ .\end{aligned} \tag{4}$$

The nonzero contributions appear only when $0a,ab,\ldots,f0$ form a sequence of nearest neighbors. There must be closed chains starting and finishing at site 0. Thus μ_m can be calculated by counting the number of such chains of length m.

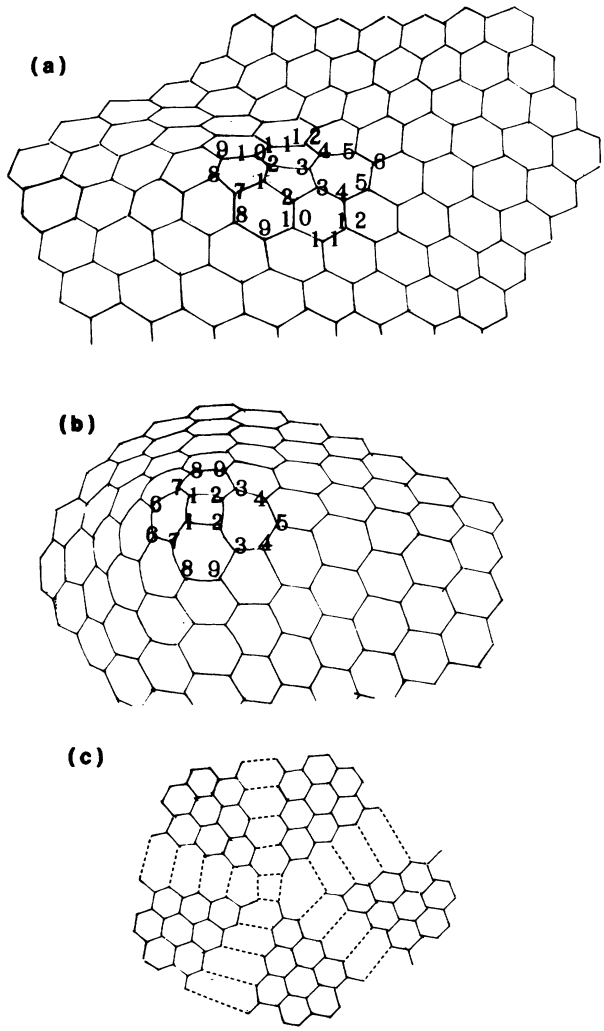

FIG. 4. (a) Fused disclination pair consisting of a five-membered ring and a seven-membered ring. Except for the sites 1, 6, and 7, there are two equivalent sites due to a mirror symmetry. (b) Fused disclination pair consisting of a four-membered ring and a seven-membered ring. There are two equivalent sites, except site 5 due to a mirror symmetry. (c) The way of connecting five sectors in order to form fused disclinations consisting of a four-membered ring and a seven-membered ring.

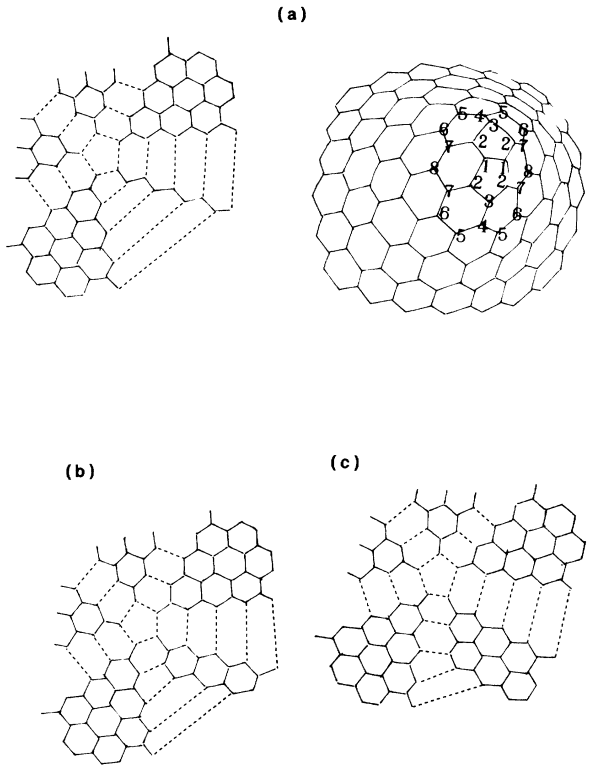

FIG. 5. Disclination pair consisting of two five-membered rings. The configuration is (1,0) for (a), (2,0) for (b), and (3,0) for (c). The way of connecting the sectors in order to form each system is shown. Because the system shown in (a) has two mirror planes, there are four equivalent sites 2, 5, 6, and 7, and two equivalent sites 1, 3, 4, and 8.

In the recursion method a mutually orthogonal set of states $|n\}$ is introduced by the following procedure:

$$\begin{aligned} |1\} &\overset{\text{def}}{=} |0\rangle \ , \\ |2\} &\overset{\text{def}}{=} H|1\} - a_1|1\} \ , \\ |n+1\} &\overset{\text{def}}{=} H|n\} - a_n|n\} - b_{n-1}|n-1\} \quad (n \geq 2) \ . \end{aligned} \tag{5}$$

In the above a_n and b_{n-1} can be determined from the condition $\{n|n+1\} = \{n-1|n+1\} = 0$, which entails $\{r|n\} = 0$, for $r < n-1$.

With the use of the normalized state $|\hat{m}\}$, the matrix element H_{nm} is defined as

$$|\hat{n}\} \overset{\text{def}}{=} |n\} / \sqrt{\{n|n\}} \ , \tag{6}$$

$$H_{nm} \overset{\text{def}}{=} \{\hat{n}|H|\hat{m}\} \ . \tag{7}$$

The following relations can be demonstrated easily:

$$H_{nn} = \frac{\{n|H|n\}}{\{n|n\}} = a_n \ , \tag{8}$$

$$H_{n-1,n} = H_{n,n-1} = (b_{n-1})^{1/2} = \frac{\{n|n\}^{1/2}}{\{n-1|n-1\}^{1/2}} \ , \tag{9}$$

$$H_{n,m} = 0 \quad (\text{for } |n-m| > 1) \ . \tag{10}$$

The matrix element H_{nm} corresponds to that of the Hamiltonian of a fictitious linear chain of "atoms" with local orbital $|\hat{n}\}$, diagonal energy a_n, and overlap matrix elements $b_n^{1/2}$ with the "atom" $n+1$. By the set $|\hat{n}\}$, μ_m can be counted as

$$\mu_m = \sum_{n_1, n_2, \ldots, n_{m-1}} \{\hat{1}|H|\hat{n}_1\} \times \{\hat{n}_1|H|\hat{n}_2\} \cdots \{\hat{n}_{m-1}|H|\hat{1}\} \ . \tag{11}$$

Then we find that, for any given length, the contributions of the closed walks to the original lattice and to the weighed linear chain are the same. It is convenient to resolve a closed path into irreducible paths which do not return to atom 0 at any of the intermediate steps. For example, $\mu_3 = \hat{\mu}_3 + 2\hat{\mu}_2\hat{\mu}_1 + \hat{\mu}_1^3$. Here $\hat{\mu}_r$ is the sum of irreducible paths of length r. For the one-dimensional case, it is easy to handle irreducible paths because looping back paths do not exist in contrast to two- or three-dimensional cases. Then $G_{00}(E)$ is given by the following recursion formula:

$$G_{00}(E) = \frac{1}{[E - a_1 - b_1 g_1(E)]} \ , \tag{12}$$

$$\begin{aligned} g_1(E) &= \frac{1}{[E - a_2 - b_2 g_2(E)]} \ , \\ &\vdots \\ g_{n-1}(E) &= \frac{1}{[E - a_n - b_n g_n(E)]} \ . \end{aligned} \tag{13}$$

The above procedure can be continued to any desired value of n. When a_n and b_n have settled down to an essentially constant value after $n\max$ steps of the above process, we can terminate this process with Eq. (14):

$$g_{n\max-1}(E) = \frac{(E - a_{n\max})}{2b_{n\max}} \left\{ 1 - \left[1 - \frac{4b_{n\max}}{(E - a_{n\max})^2} \right]^{1/2} \right\} . \tag{14}$$

Once the Green's function is calculated by the above process, the LDOS at a particular site is given by Eq. (2). The imaginary part comes from the square root in Eq. (14). We have summed over all irreducible paths of length up to $2n\max$ and all reducible paths that can be built up out of these. So, the first $2n\max$ moments of $N_0(E)$ remain exact. In this paper, we take $n\max$ to be 190.

III. ELECTRONIC STRUCTURE OF THE DISCLINATION

A. General feature

Our tight-binding model has no quantitative disorder. Every atomic site has a fixed coordination number z, i.e., the number of nearest neighbors is three. The Schrödinger equation becomes

$$-T\sum_j a_j = Ea_i \ . \tag{15}$$

Here $\sum_j$ represents the summation over j which is confined to the nearest neighbors of i. a_i represents the amplitude of the eigenfunction at site i. Suppose that i labels the site where this eigenfunction has the maximum amplitude; then $|E| \le T\sum_j |a_j|/|a_i| \le zT$, i.e., all the states must lie within the band. So the sum rule

$$\int_{-zT}^{zT} dE\, N_0(E) = 1 \tag{16}$$

holds with an excellent numerical accuracy in all the cases in this paper.

The state corresponding to $E=-zT$ is a bonding state, which is realized when the amplitude a_i of all sites i have the same sign and the same magnitude. This state forms the lowest-energy state in the band for all the cases in this paper.

On the other hand, the state corresponding to $E=zT$ is an antibonding state, and is realized when all coefficients a_i and a_j, with i and j being nearest-neighbor sites, have the same magnitude and opposite sign. In this case a_i must alternate in sign around every ring of the network. This is possible for even-membered rings, but not for odd-membered rings. In an odd-membered ring, it is inevitable that sites having amplitude of the same sign become nearest neighbors. We call such a situation a "frustration." The effect of odd-membered rings is more significant to the antibonding states than to the bonding states due to the frustration.

Now we consider the moment which corresponds to the number of closed paths. A perfect lattice can be divided into sublattices, consisting of A and B sites, in a way such that all A sites are connected only to B sites, and vice versa. This will be called a sublattice structure in the following. In the sublattice structure, the closed path takes the form $A\to B\to A\to B\to\cdots A$, and its length is necessarily even. Therefore all the odd moments are zero, and the LDOS has a symmetric shape with respect to $E=0$. This is easily understood considering the relation between the shape of the LDOS and the moment μ_m represented by $\mu_m=\int_{-\infty}^{\infty} dE N_0(E)E^m$. However, if an odd-membered ring exists, the system cannot be divided into sublattices. Connections between A and A, or B and B, necessarily occur because there are closed paths with odd length which wind around the odd ring an odd number of times. Odd moments are not zero, so the LDOS is not symmetric with respect to the origin of the energy.

Figure 6 shows the sectors described in Sec. II for the 5 system on the left, and for the 6 system (perfect graphite lattice) on the right. Consider a closed path starting and finishing at site zero in both systems. If a path in one system has the same local geometry as a path in another system, we will say that the two paths correspond to each other.

The winding number is defined as follows. If a closed path in an n system winds around an n ring n_r times clockwise, and n_l times counterclockwise, then its winding number is n_r-n_l. Here an n ring means the n-membered ring formed by apexes of the isosceles triangle

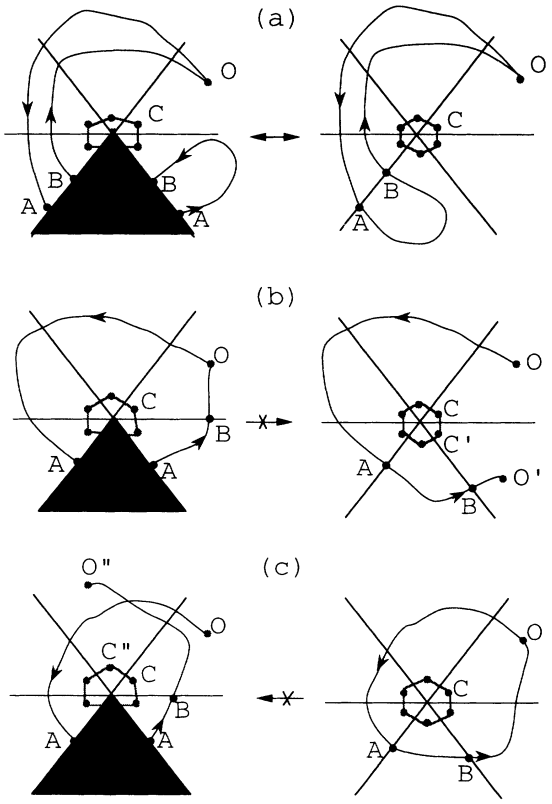

FIG. 6. The correspondence between the closed path of 5 system and that of perfect graphite lattice. The 5 system is shown on the left and the perfect lattice is shown on the right. The shaded area in the left represents the removed sector. The configuration for C and O is the same as that for C' and O' in (b) and that for C'' and O'' in (c) if the sector is rotated by $\pi/3$ clockwise or counterclockwise, respectively. The paths in one system have the same local geometry as those in another system.

sector in an n system. For closed paths whose winding number is zero, there is one-to-one correspondence between both systems [see Fig. 6(a)], while for a closed path in the 5 system whose winding number is neither zero nor a multiple of six, the corresponding path in the 6 system does not close [see Fig. 6(b)]. Therefore the moment of the 5 system corresponding to this path increases compared to that of the 6 system. It is also true if we exchange 5 and 6 in the above sentences [see Fig. 6(c)]. It is the paths winding around the n ring or the 6 ring that change the LDOS of the n system as compared to that of the 6 system.

B. Single disclination; n system

Figure 7(a) shows the LDOS at the C atom in the five- and the seven-membered rings in n systems ($n=5$ and 7), compared with the perfect lattice. For an n system with odd n, since it does not have a sublattice structure, the shape of the LDOS is not symmetric with respect to the origin of the energy. For the five-membered ring the LDOS is reduced in the energy region between $0.4T$ and T, and increased between $-T$ and 0 as compared with

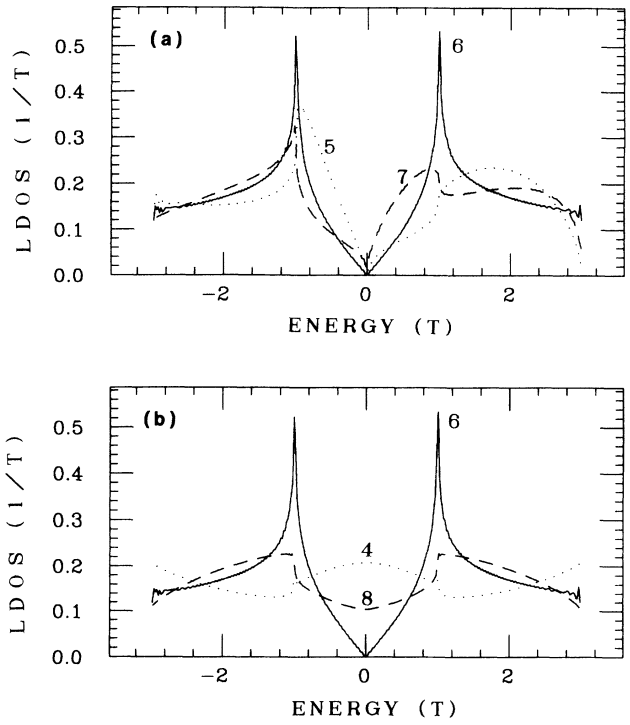

FIG. 7. The LDOS at the site of the single disclination center in n systems. The attached number shows n.

that of the perfect lattice. Roughly speaking, the LDOS of the 7 system is enhanced where that of the 5 system is reduced, and vice versa. Thus it resembles that of the 5 system if the direction of energy axis is reversed.

At the Fermi level E_F, where E_F is chosen as the origin of the energy, the sharp V-shaped valley structure is kept for both five- and seven-membered rings, and the LDOS value vanishes exactly at E_F. If we look more closely into the change of the spectra near E_F, a significant increase of the absolute value of the gradient at E_F can be found. This would indicate the appearance of resonant states around the Fermi level.

At the energies where the LDOS of the perfect lattice shows the logarithmic divergence, i.e., $E=\pm T$, the divergence disappears for the n system ($n=5,7$). But the derivative becomes divergent when E approaches T from lower energy when $n=5$, and from higher energy when $n=7$.

To see the spatial extent of the distorted LDOS spectra due to the disclination, the LDOS's are calculated for each atom site around the n ($n\neq 6$)-membered ring. The results are shown in Figs. 8 and 9 for the case of the five-membered ring and the seven-membered ring, respectively. The label of the atom site attached to the spectrum is illustrated in Fig. 2(b).

On the second carbon ring (-2-3-2-2-3-2-) measured from the center of n ($n\neq 6$)-membered ring, the distortion of the spectra at the disclination center is already considerably reduced. In particular, the spectral feature of the van Hove singularity at $\pm T$ is already recovered. On the third carbon ring (-4-5-6-5-4-4-5-6-5-4-), the distortion of the LDOS from the perfect 2D crystal is further reduced, though we still notice some significant modification as compared with the perfect one. A clear shoulder structure appears in the third ring at an energy slightly higher than the Fermi level ($E=0$) for the case of the 7 system, and at an energy slightly lower than the Fermi level for the case of the 5 system. This indicates a well-defined resonant state.

In the energy region deeper than the saddle-point energy ($E<E_F-T$, $E_F+T<E$), an oscillatory behavior of the spectra is found. The period of the oscillation becomes shorter on going to the outer carbon rings, as is shown by a comparison of the oscillations for the LDOS of $1\rightarrow 2,3\rightarrow 4,5,6\rightarrow 7,8,9,10$. This feature can be explained by the interference of the incoming and outgoing radial wavefunction to the n ($n\neq 6$)-membered ring. The amplitude of the oscillation in the region $E>T$ is larger than that in the region $E<-T$. This is due to the frustration.

Figure 7(b) shows the LDOS at the C atom in the $n=$

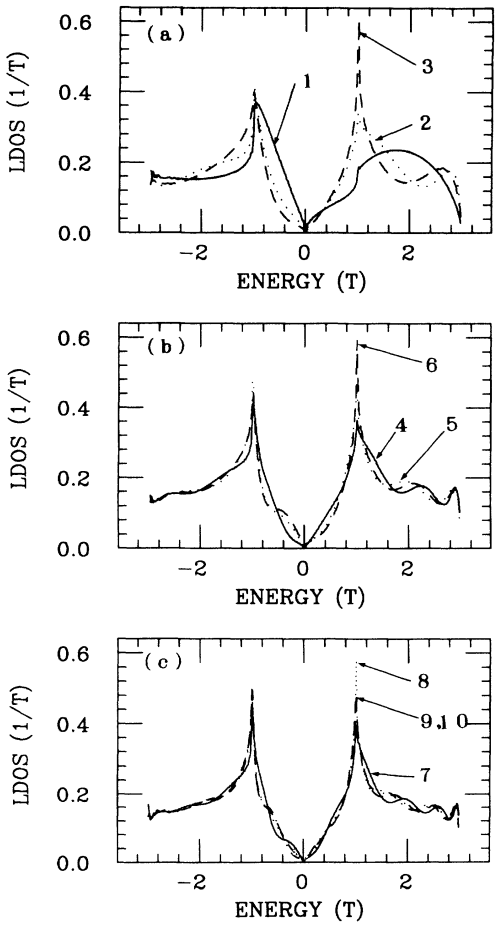

FIG. 8. The LDOS's at sites around the disclination center of the 5 system. The LDOS's of sites 1, 4, and 7 are shown by real lines, those of sites 2, 5, and 8 by dotted lines, those of the sites 3, 6, and 9 by dashed lines, and that of site 10 by a dot-dashed line, respectively. The labels of sites are shown in Fig. 2(b). (a) The first and the second rings. (b) The third ring. (c) The fourth ring.

four-, and eight-membered rings in n systems, compared with that of the perfect lattice. Since an n system with even n has a sublattice structure, the LDOS has a symmetric shape with respect to E_F. A remarkable feature for these cases is that the LDOS takes a finite value at E_F, and the sharp V-shaped valley feature disappears. This is quite different from the LDOS for odd n systems or for the perfect 2D graphite lattice. The states contributing to the finite LDOS around E_F is localized in space, which can be confirmed by inspection of LDOS's for various C sites around the disclination center. Figures 10 and 11 show examples of 4 and 8 systems, respectively. By going to outer carbon-atom rings, the LDOS around E_F is reduced, and, for the fourth rings from the disclination, almost the same V-shaped spectrum of the perfect lattice is recovered, though a finite value of the LDOS remains at E_F. The recovery of the sharp peak of the logarithmic singularity is attained already in the second carbon ring as in the case of the 5 and 7 systems.

The ripple shape of the spectra in the deeper energy region ($E < E_F - T$, $E > E_F + T$) is smaller for the case of the saddle point-disclination center (an n system, $n > 6$) than for the case of the conical point disclination center (an n system, $n < 6$).

C. Fused disclinations and disclination pair; n-m system

Proximity of two disclinations, especially fused disclinations, causes a more drastic change of electronic states as compared to a single $n\,(n \neq 6)$-membered ring of an n system. Here fused disclinations of n- and m-membered rings creates an n-m system whose configuration is (1,0), following the definition in Sec. II. Such fused disclinations might be generated in the process of the growth of the carbon nanostructure.[7] We have calculated electronic states for various combinations of fused $n\,(n \neq 6)$-membered rings. Figure 12 shows LDOS's at various sites for fused disclinations of five- and seven-membered rings, i.e., the 5-7 system. The label attached to each spectrum corresponds to the site shown in Fig. 4(a).

Sites 1–6 belong to fused five- and seven-membered rings. The spectra on these sites are remarkably changed from those of the perfect 2D lattice. In particular, the spectra for sites 1, 3, and 6 show no trace of a peak at $E = T$. However, with the increase of the distance from the defect center, a rapid recovery of the spectra to the perfect one can be observed.

Of special interest in the electronic state of this system

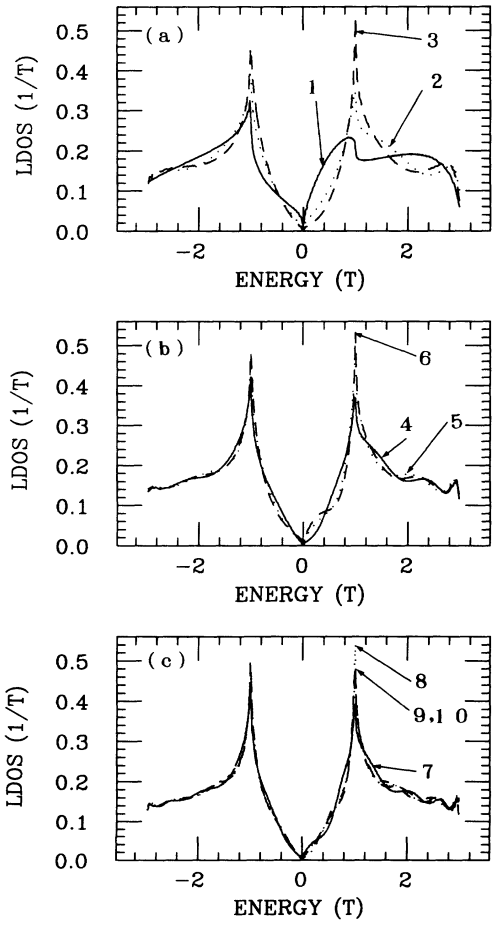

FIG. 9. The LDOS's at the sites around the disclination center of the 7 system. The correspondence between the types of lines and labels of sites is the same as in Fig. 8. (a) The first and second rings. (b) The third ring. (c) The fourth ring.

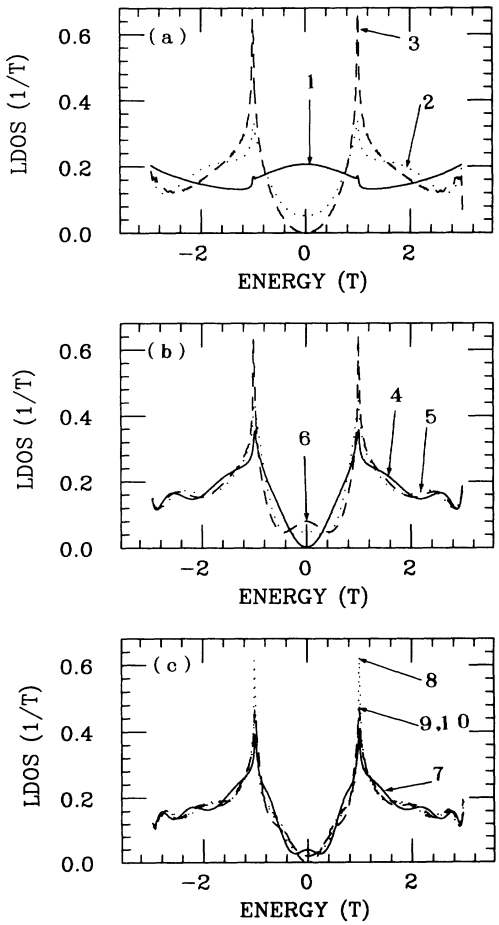

FIG. 10. The LDOS's at the sites around the disclination center of the 4 system. The correspondence between the types of lines and labels of sites is the same as in Fig. 8. (a) The first and the second rings. (b) The third ring. (c) The fourth ring.

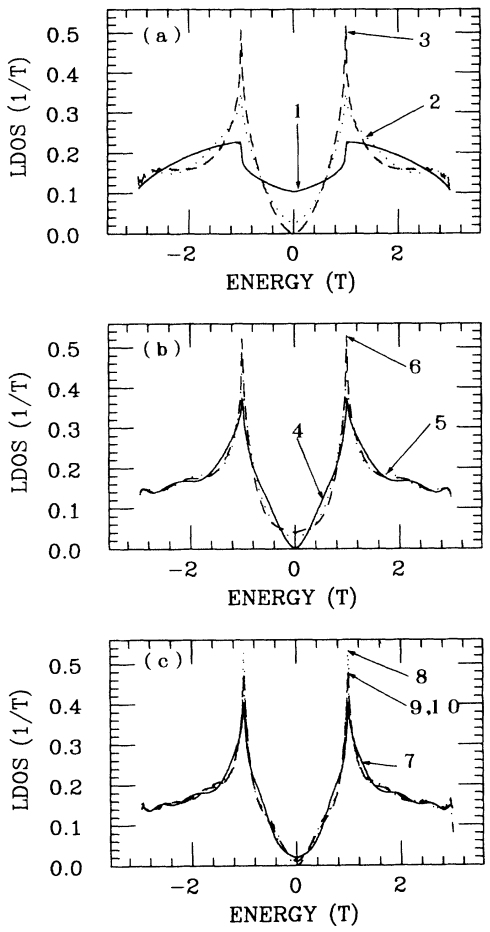

FIG. 11. The LDOS's at the sites around the disclination center of the 8 system. The correspondence between the types of lines and labels of sites is the same as in Fig. 8. (a) The first and the second rings. (b) The third ring. (c) The fourth ring.

is the emergence of two sharp resonant states near the Fermi level. That is to say, a clear peak structure appears for sites 1 and 3 at an energy slightly higher than E_F, i.e., at about $0.2T$, and another peak appears at site 5 slightly below E_F ($\simeq -0.2T$). The former peak is caused by the seven-membered ring, and the latter by the five-membered ring. Although site 2 is nearer to the seven-membered ring than site 1, and site 4 is nearer to the five-membered ring than site 5, these peaks do not appear at sites 2 and 4. The LDOS's at sites 7 and 8 and at site 6 are approximately the same as those at sites 3 and 2 of the 5 system, and that at site 1 of the 7 system, respectively. But a small shoulder appears near E_F for site 8.

The fused disclinations of four- and seven-membered rings, i.e., the 4-7 system, entails a much sharper peak at an energy position very close to E_F, as seen in Fig. 13. The labels for the spectra correspond to the carbon sites shown in Fig. 4(b). The strongest intensity of the resonant peak is found at site 2. But the intensity is partially shared by sites 1, 4, 6, and 8, and so on. Figure 14 shows this peak's height, and Fig. 15 shows the energy of the peak's center for various $n$max. The attached numbers indicate locations of the sites shown in Fig. 4(b). The square root of the peak's height corresponds to the absolute value of the wave function, i.e., the absolute value of the coefficients a_i in Eq. (15). The sign of a_i can be found by matrix diagonalization. It can be seen from the sign that the wave function is antisymmetric with respect to the symmetry line. Therefore the LDOS at site 5, which is located on the symmetry line, does not have this peak, and the value of the LDOS vanishes at E_F. As $n$max increases, the peak's height increases, the width becomes narrower, and the peak's center approaches the origin of the energy. The increase of the peak height indicates that the state is a localized state, and its wave function decays upon leaving from the disclination pair, i.e., the four- and

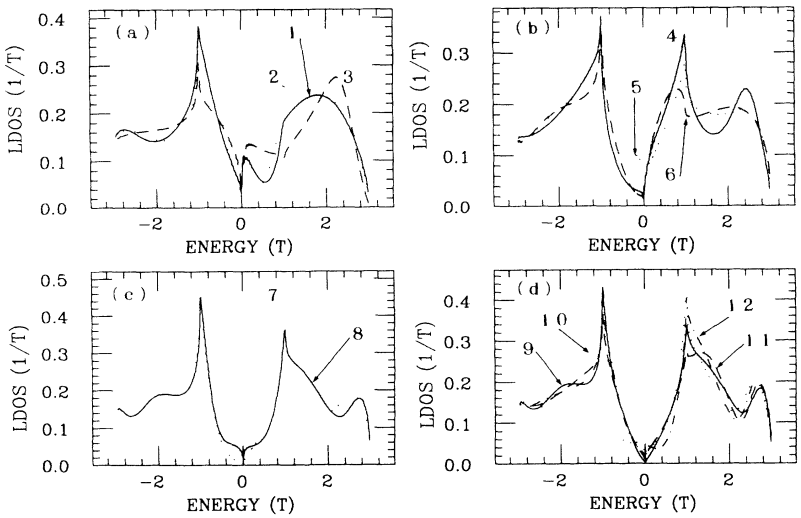

FIG. 12. The LDOS's of the 5-7 system with configuration (1,0). The LDOS's of sites 1, 4, 8, and 9 are shown by real lines, those of sites 2, 5, 7, and 10 by dotted lines, those of sites 3, 6, and 11 by dashed lines, and that of site 12 by a dot-dashed line, respectively. The attached labels of sites are shown in Fig. 4(a). (a) The five-membered ring. (b) The seven-membered ring. (c) and (d) The second ring.

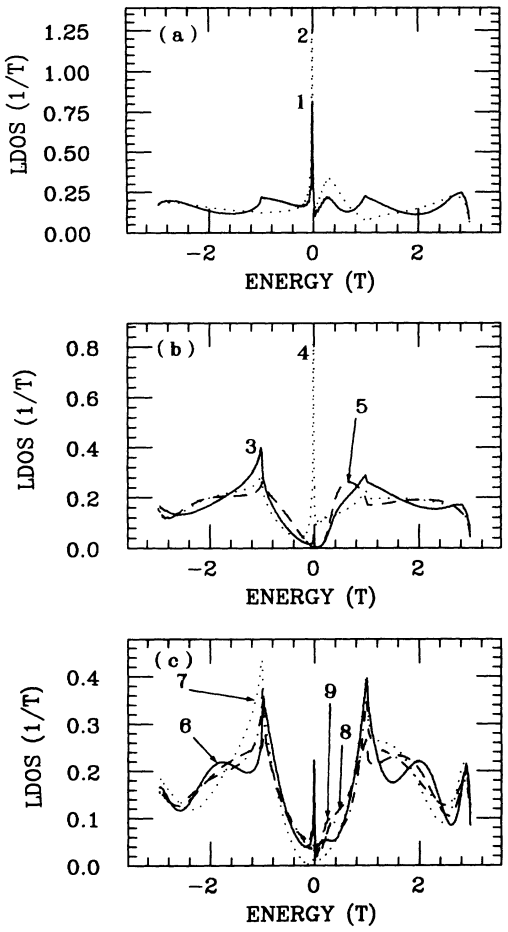

FIG. 13. The LDOS's of 4-7 system with configuration (1.0). The LDOS's of sites 1, 3, and 6 are shown by real lines, those of sites 2, 4, and 7 by dotted lines, those of sites 5 and 8 by dashed lines, and that of site 9 by a dot-dashed line. The attached labels of sites are shown in Fig. 4(b). (a) The four-membered ring. (b) The seven-membered ring. (c) The second ring.

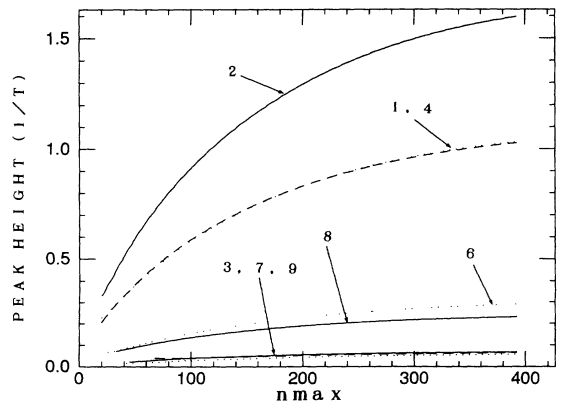

FIG. 14. The height of the sharp peak around the Fermi level in the LDOS of a 4-7 system with configuration (1,0) vs $n$max. The attached labels for the sites are shown in Fig. 4(b).

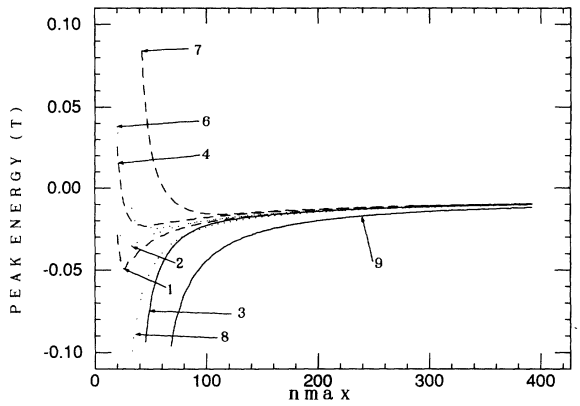

FIG. 15. The energy of the sharp peak around the Fermi level in the LDOS of a 4-7 system with configuration (1,0) vs $n$max. The attached labels for the sites are shown in Fig. 4(b).

the seven-membered rings. Information about the degree of the spatial localization of this state can be derived by the analysis of the $n$max dependence of the peak. We discuss details about this in a forthcoming paper. We also calculate the LDOS of the fused disclinations in n-m systems so far as n is 4~12 and m is 5~12. Then the sharp peak near $E-0$ similar to that of the 4-7 system appears in other n-m systems if n is a multiple of 4, i.e., $n=4$, 8, or 12, and m is an odd number, i.e., $m=5$, 7, 9,

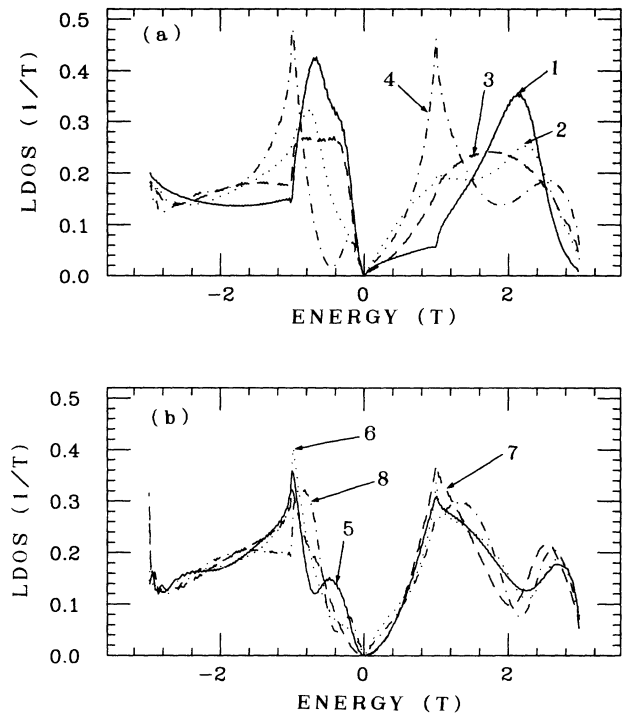

FIG. 16. The LDOS's of a 5-5 system with configuration (1,0). The LDOS's of sites 1 and 5 are shown by real lines, those of sites 2 and 6 by dotted lines, those of sites 3 and 7 by dashed lines, and those of sites 4 and 8 by dot-dashed lines. The attached labels of sites are shown in Fig. 5(a). (a) Sites 1, 2, 3, and 4. (b) Sites 5, 6, 7, and 8.

or 11. But the peak's height becomes smaller as n and m increase.

Figure 16 shows the LDOS of a 5-5 system with configuration (1,0). The label attached to each spectrum corresponds to the location of sites indicated in Fig. 5(a). The value of the LDOS vanishes at E_F as in the case of 5 system. The sharp peak structure at $E=-T$ disappears for sites 1, 3, and 8. In particular, the LDOS at site 3 is nearly constant between $E=-T$ and $-0.4T$. But the value of the derivative for these sites changes discontinuously from nearly zero to a large positive one when E approaches $-T$ from the lower energy. A clear peak structure appears at slightly below E_F for sites 4, 5, and 8. It corresponds to the shoulder structure in the 5 system.

So far we have discussed the electronic states of the fused disclinations. What then happens when the two disclination centers are gradually separated to the infinite distance? Figure 17 shows LDOS's near E_F for the 4-7 and 5-5 systems for various configurations. The attached pair of integers (i,j) represents the configuration of two disclination centers (see Fig. 3). The site for the LDOS is indicated by the circle in Fig. 3. For the 4-7 system, the location of the four-membered ring is taken as (0,0). When $i-j$ is not a multiple of 3, the feature of the LDOS near the Fermi energy resembles that of the fused disclinations; the peak structure appears at $E=E_F$ for the 4-7 system, while the values of the LDOS vanishes there for the 5-5 system. As the two disclinations separate from one another, the shapes of the LDOS's of the disclination pair approach those of the single disclination, e.g., the sharp peak of the 4-7 system becomes lower.

But when $i-j$ is a multiple of 3, the feature is drastically changed; the peak structure vanishes at $E=E_F$ for the 4-7 system and the LDOS takes a finite value for the 5-5 system. For 4-7 system, two dull peaks, instead of a sharp peak, appear below and above E_F. As the two disclinations separate from each other, centers of the two dull peaks of the 4-7 system approach E_F, with their width becoming narrower, while the finite value at E_F of a 5-5 system decreases. Thus the shapes of the LDOS's also approach those of the single disclination, but the method of approach is different from those for the case of $i-j$, not being a multiple of 3. Such a relation between the peak at E_F and the configuration of the disclination pair is also observed in other n-m systems which have a peak similar to that of 4-7 system, i.e., $n=4$, 8, and 12, and $m=5$, 7, 9, and 11. Though the double disclination system, i.e., an n-m system, does not have any translational symmetry, this condition on $i-j$ resembles the condition about the screw axis of a carbon nanotube which determines whether the nanotube is a metal or a semiconductor.[7]

IV. CHARGE AND STABILITY

We have seen that sites distant from disclination(s) have the same LDOS as that of the 2D graphite. Therefore, in an infinite system there are infinite sites which have the same LDOS as that of the graphite. As the total DOS is the average of LDOS's of every site, the total DOS agrees with that of the graphite. So the Fermi level coincides with that of graphite, i.e., zero.

The charge of a site is given by

$$-2\int_{-3}^{0} dE\{N_0(E)-N(E)\} . \tag{17}$$

Here $N_0(E)$ is the LDOS of the site, and $N(E)$ is that of the graphite. The unit of charge is the absolute value of an electron's charge. Because $N(E)$ is an even function of the energy, we confirm that $\int_{-3}^{0} dE\, N(E)=0.5$.

The stability energy of a site compared to the perfect graphite site is represented by

$$-2\int_{-3}^{0} dE\, E\{N_0(E)-N(E)\} . \tag{18}$$

If a site has a large negative stability energy, we will say that the site is unstable compared to the graphite. Factor

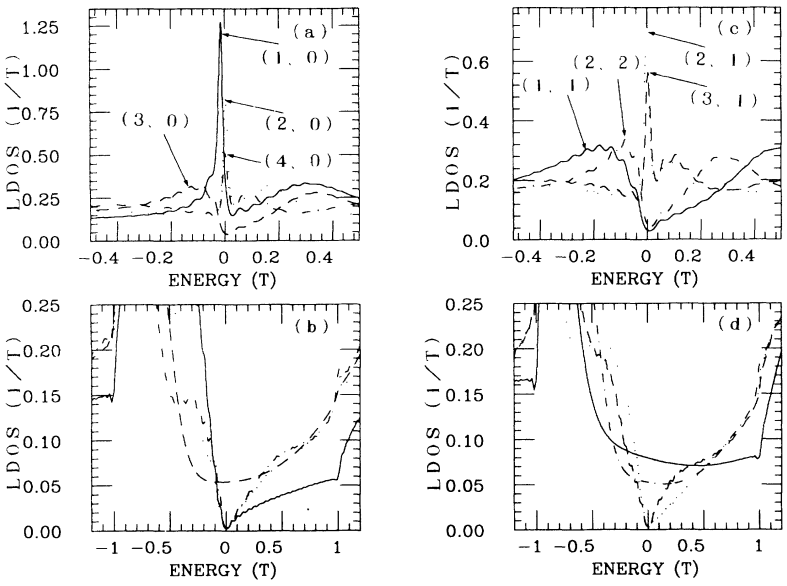

FIG. 17. The LDOS's of 4-7 and 5-5 systems near Fermi energy about various configurations. The LDOS's of configurations (1,0), (2,0), (3,0), and (4,0) are shown by real, dotted, dashed, and dot-dashed lines, respectively, in (a) and (b). The LDOS's of configurations (1,1), (2,1), (3,1), and (2,2) are shown by real lines, dotted lines, dashed lines, and dot-dashed lines, respectively, in (c) and (d). The LDOS's of a 4-7 system are shown in (a) and (c), and those of a 5-5 system are shown in (b) and (d).

TABLE I. The charge and stability energy calculated by the LDOS at each site in the 5-7 system with the configuration (1,0). The labels of the sites are shown in Fig. 4(a). The unit of the charge is the absolute value of an electron charge, and that of the stability energy is the absolute value of the transfer-matrix element, i.e., T. The charge and stability energy of the sites whose labels do not appear in Table I are so small that they cannot be determined clearly.

Site	1	2	3	4	5	6	7
charge	−0.05	−0.08	−0.04	0.06	0.02	0.04	0.02
stability	−0.02	−0.01	−0.04	−0.02	−0.02	− 0.02	0.00

2 in Eqs. (17) and (18) represents spin multiplicity. For the case of an n system which has a single disclination, the charge and stability energy are almost the same as those of the perfect 2D graphite except at the n-membered ring and at site 3 in the 4 system. The charges at the five- and seven-membered rings is -0.07 and $+0.04$ respectively. The charges of n systems with even n are zero because of the symmetric shape of their LDOS. The stability energies at the four-, five-, seven-, and eight-membered rings are $-0.11T$, $-0.02T$, $-0.02T$, and $-0.02T$, while that at site 3 in the 4 system is $+0.02T$.

From the analysis of the charge, it seems that the five-membered ring behaves attractively, and the seven-membered ring behaves repulsively to the electrons. As for the stability energy, the four-membered ring is especially unstable.

The charge and the stability energy for the 5-7, 4-7, and 5-5 systems are listed in Tables I, II, and III, respectively. They are compared with those of n-membered rings in a single disclination, which will be called simply n-membered rings in what follows. The sites between two disclinations become the most unstable. For the 5-7 system, sites 2 and 6 have almost the same charge as the five-membered ring and the seven-membered ring, respectively. Sites 1 and 3 are less negative than the five-membered ring because of the resonant state above F_F. Compared to the seven-membered ring, site 5 is less positive on account of the resonant peak below E_F, and site 4 is more positive. For the 4-7 system, sites 2, 3, 4, and 5 are less positive than the seven-membered ring. For the 5-5 system, sites 1 and 3 are more negative, and site 2 is less negative than the five-membered ring.

We should comment that these calculations do not include the effect of mixing between the σ and π bands, and the interaction between electrons, which are needed for a quantitative discussion of realistic systems.

TABLE II. The charge and the stability energy calculated by the LDOS of each site in the 4-7 system with the configuration (1,0). The labels of the sites are shown in Fig. 4(b). The unit of the charge and that of the stability energy are the same as those of Table I. The charge and stability energy of the sites whose labels do not appear in Table II are so small that they cannot be determined clearly.

Site	1	2	3	4	5	6	8
charge	−0.02	0.00	0.02	0.01	0.02	0.00	0.00
stability	−0.11	−0.14	0.00	−0.04	−0.02	−0.01	−0.02

TABLE III. The charge and stability energy calculated by the LDOS of each site in the 5-5 system with the configuration (1,0). The labels of the sites are shown in Fig. 5(a). The unit of the charge and that of the stability energy are the same as those of Table I. The charge and stability energy of the sites whose labels do not appear in Table III are so small that they cannot be determined clearly.

Site	1	2	3	5	7	8
charge	−0.15	−0.05	−0.10	−0.02	0.00	−0.02
stability	−0.04	0.00	−0.02	0.00	+0.02	0.00

V. CONCLUSION AND DISCUSSION

In the present paper, the electronic structure of the disclination center, i.e., the $n(\neq 6)$-membered ring, inserted in the otherwise perfect 2D graphite lattice is obtained by the recursion method. In the present treatment only the π band is treated with the tight-binding model, only with nearest-neighbor hopping interaction. It was found that the LDOS is drastically distorted on the $n(\neq 6)$-membered ring, but is quickly recovered to the normal LDOS with the increase of the distance from the disclination center(s). This result is natural since a distant defect affects only the higher moment in the LDOS curve. At the Fermi energy, the LDOS of an n-membered ring in an n system with $n=5$ and 7 is zero, and that with $n=4$ and 8 remains a finite value. The drastic change of the local electronic structure of the $n(\neq 6)$-membered ring entails a special electronic property of these sites, for instance, the distortion of the structure, chemical reactivity, or the electron emission capability. The microscopic shape of the curved graphite surface around the disclination center, e.g., the bending angle of the bond connecting the $n(\neq 6)$-membered ring to the remaining bulk part, could only be discussed by arguments taking into account the σ bond. The necessity of this is also made clear by the breakdown of the pure sp^2 hybridization scheme. The theoretical calculation of the structure optimization by the first-principles local-density approximation (LDA) is worthwhile, and is our next project to be undertaken.

In the present work various strange resonant states were found. The sharp peak near $E=0$ of the 4-7 system and so on will be particularly interesting for the application to the coherent electron emission source, when used as a field emitter. The reason is that the contribution from this peak is dominant, so that almost an ideal monocromaticity of emitted electrons will be realized. Such a sharp peak state is also important for an ambiguous quantitative analysis of scanning tunneling microscopy (STM) and spectroscopy (STS). This is because tunneling current is contributed by the electronic states in the energy region of the Fermi level offset between the tip and the surface. Thus, for a quantitative analysis of the STS, deconvolution of the surface and tip electronic structure is inevitable, which obscures the results obtained. However, if the electron tunneling takes place via a single en-

ergy level of the tip, the deconvolution is trivial, and the differential tunnel conductance solely reflects the surface electronic states of the corresponding energy position. Various interesting phenomena such as local negative tunnel conductance are easily realized. Realization that the above-mentioned portion of the carbon nanostructure is the tip of the STM or field emitter is highly interesting.

The various configuration of a disclination pair other than the fused case is also investigated for the 4-7 and 5-5 systems. When the configuration satisfies a certain simple condition, the feature is drastically changed compared to the case of the fused disclinations, i.e., at $E=E_F$, the peak structure vanishes for the 4-7 system, and a finite value of the LDOS remains for the 5-5 system. This condition is expected to have some relation to that of a screw axis of carbon nanotube, which determines whether the nanotube is a metal or a semiconductor.[7] As for the charge calculated from the LDOS of a single disclination center, the five-membered ring has a negative charge, the seven-membered ring has a positive one, and even-membered rings are neutral. That is to say, the five-membered ring is attractive and the seven-membered ring is repulsive to electrons. This tendency is kept approximately for the fused disclinations. The disclination centers of the five-membered and seven-membered rings are certainly realized in fullerenes and nanotubes. Though no experimental evidences have been reported so far for fused disclinations, such a type of defect may exist for the growth process.[7,9] Therefore the study of the chemical properties of such defects seems to be important.

ACKNOWLEDGMENTS

This work is supported by Grant-in-Aid for Scientific Research from Ministry of Education, Science and Culture.

[1]D. Ugarte, Nature (London) **359**, 707 (1992).
[2]M. Fugita, R. Saito, M. S. Dresselhaus, and G. Dresselhaus, Phys. Rev. B **45**, 13 834 (1992).
[3]S. Iijima, T. Ichihashi, and Y. Ando, Nature (London) **356**, 776 (1992).
[4]Y. Irie and K. Kawamura, Prog. Theor. Phys. **70**, 674 (1983).
[5]Y. Nagaoka and M. Ikegami, in *Transport Phenomena in Mesoscopic Systems,* edited by H. Fukuyama and T. Ando (Springer-Verlag, Berlin, 1992), p. 167.
[6]K. Kitahara, H. Araki, and K. Nakazato, in *Dislocation in Solids,* edited by H. Suzuki, T. Ninomiya, K. Sumino, and S. Takeuchi (University of Tokyo Press, Tokyo, 1985), p. 117.
[7]M. S. Dresselhaus, G. Dresselhaus, and R. Saito, Solid State Commun. **84**, 201 (1992).
[8]R. Haydock, V. Heine, and M. J. Kelly, J. Phys. C. **5**, 2845 (1972).
[9]R. Saito, G. Dresselhaus and M. S. Dresselhaus, Chem. Phys. Lett. **195**, 537 (1992).

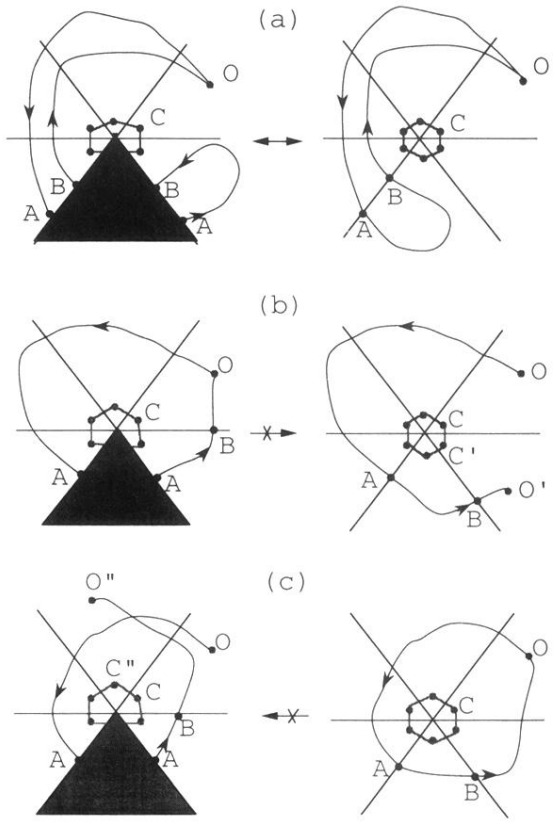

FIG. 6. The correspondence between the closed path of 5 system and that of perfect graphite lattice. The 5 system is shown on the left and the perfect lattice is shown on the right. The shaded area in the left represents the removed sector. The configuration for C and O is the same as that for C' and O' in (b) and that for C'' and O'' in (c) if the sector is rotated by $\pi/3$ clockwise or counterclockwise, respectively. The paths in one system have the same local geometry as those in another system.